Primordial density and BAO reconstruction

Hong-Ming Zhu,[1,2] Ue-Li Pen,[3,4,5,6] and Xuelei Chen[1,2,7]

[1] *Key Laboratory for Computational Astrophysics, National Astronomical Observatories, Chinese Academy of Sciences, 20A Datun Road, Beijing 100012, China*
[2] *University of Chinese Academy of Sciences, Beijing 100049, China*
[3] *Canadian Institute for Theoretical Astrophysics, University of Toronto, 60 St. George Street, Toronto, Ontario M5S 3H8, Canada*
[4] *Dunlap Institute for Astronomy and Astrophysics, University of Toronto, 50 St. George Street, Toronto, Ontario M5S 3H4, Canada*
[5] *Canadian Institute for Advanced Research, CIFAR Program in Gravitation and Cosmology, Toronto, Ontario M5G 1Z8, Canada*
[6] *Perimeter Institute for Theoretical Physics, 31 Caroline Street North, Waterloo, Ontario, N2L 2Y5, Canada*
[7] *Center of High Energy Physics, Peking University, Beijing 100871, China*

(Dated: November 13, 2016)

We present a new method to reconstruct the primordial (linear) density field using the estimated nonlinear displacement field. The divergence of the displacement field gives the reconstructed density field. We solve the nonlinear displacement field in the 1D cosmology and show the reconstruction results. The new reconstruction algorithm recovers a lot of linear modes and reduces the nonlinear damping scale significantly. The successful 1D reconstruction results imply the new algorithm should also be a promising technique in the 3D case.

PACS numbers:

I. INTRODUCTION

The observed large-scale structure of the Universe, which contains a wealth of information such as the nature of dark energy, neutrino masses, and primordial power spectrum etc, is a powerful probe of cosmology. The matter power spectrum has been measured to significant accuracy in the current galaxy surveys and the precision will continue to improve with future surveys. However, the nonlinear gravitational evolution is a complicated process and makes it difficult to model the small-scale inhomogenities. This has led to many theoretical challenges in developing perturbation theories (see e.g. [1] for a brief review). On the other hand, various reconstruction techniques have been proposed to reduce nonlinearities in the density field, in order to obtain better statistics [2, 3].

The standard BAO reconstruction uses the negative Zel'dovich (linear) displacement to reverse the large-scale bulk flows [2]. The nonlinear density field is usually smoothed on the linear scale (~ 10 Mpc$/h$) to make the Zel'dovich approximation valid. Actually, the fully nonlinear displacement which describes the motion beyond the linear order (the Zel'dovich approximation) can be solved from the nonlinear density field. While the algorithm is complicated in the three spatial dimensions, it is quite simple in the 1D case, which is basically the ordering of mass elements (sheets). The 1D cosmological dynamics corresponds to the interaction of infinite sheets of matter where the force is independent of distance [1]. The simplified 1D dynamics provides an excellent means of understanding the structure formation and testing perturbation theories [1]. In this paper we solve the fully nonlinear displacement in 1D and present a new method to reconstruct the primordial density field and hence the linear BAO information.

This paper is organized as follows. In Section II, we present the reconstruction algorithm in the 1D case. In Section III, we briefly describe the 1D N-body simulation. In Section IV, we show the results of reconstruction. In Section V, we discuss the 3D case and future improvements.

II. RECONSTRUCTION ALGORITHM

The Lagrangian displacement $\Psi(q)$ fully describes the motion of mass elements. The Eulerian position x of a mass element is

$$x = q + \Psi(q), \tag{1}$$

where q is the initial Lagrangian position of this mass element. In simulations, mass elements (sheets) are labeled by their initial Lagrangian coordinates. Once we know their Eulerian positions, the displacement field is obtained. However, in observations we only have the unlabelled Eulerian coordinates. We can order the sheets according to their Eulerian coordinates from left to right, regardless of their initial Lagrangian coordinates. The Eulerian position of the ith sheet from the left side is x_i. The estimated displacement at the Lagrangian coordinate $q = iL/N$ is

$$s(q) = x_i - iL/N, \tag{2}$$

where we have ordered the sheet lables i from left to right, L is the box size, and N is the sheet number. Here, $q = iL/N$ is the estimated initial Lagrangian position for

the ith sheet at position x_i. If no shell crossing happens, the reconstructed displacement is exact up to a global shift. In the nonlinear regime once shell crossing occurs, the estimated displacement field is quite noisy on the scale $\sim L/N$. To reduce stochasticities in the estimated displacement field, we can use the averaged displacement of n_p particles

$$s(q) = \frac{1}{n_p} \sum_{j=i}^{i+n_p-1} x_j - in_pL/N, \tag{3}$$

where $q = in_pL/N$ and j is the sheet label. Here i varies from 0 to N/n_p and j varies from 0 to N. We take $n_p = 5$ to estimate the displacement field in this paper.

The derivative (actually the divergence) of $s(q)$ gives the reconstructed density field

$$\delta_r(q) = -\frac{\partial s(q)}{\partial q}, \tag{4}$$

i.e., the differential motion of mass elements. Reconstruction from the gridded density field can be implemented following the same principle, which we adopt in the following calculations. In this case, densities are computed on N/n_p grids, where the average density is n_p. We can calculate the averaged displacement of the first n_p particles from the gridded densities and then iterates $N/n_p - 1$ times for the next $N - n_p$ particles. This method directly gives the displacements on N/n_p grids.

III. SIMULATIONS

The 1D N-body dynamics can be simulated using the particle-mesh (PM) method. The 1D simulations we use are run with the 1D PM code in Ref. [1]. The 1D simulation involves 3×10^8 sheets with 3×10^8 PM elements in a 10^8 Mpc box. The 1D simulation assumes a matter-dominated background cosmology ($\Omega_m = 1$) and have the same dimensionless power spectrum as the concordance cosmology, i.e.,

$$kP_{\rm 1D}(k)/\pi = k^3 P_{\rm 3D}(k)/(2\pi^2), \tag{5}$$

where $P_{\rm 3D}$ is the 3D linear power spectrum from the linear Boltzman code.

The initial condition is generated using the Zel'dovich approximation. Since the Zel'dovich approximation is exact up to shell crossing, the PM calculation is started at $z = 10$. In the analysis, we use the output at $z = 0$. We also scale the initial density field by the linear growth factor to get the linear density field at $z = 0$.

Note that the nonlinear evolution in 1D is more significant than the 3D case. The nonlinear evolution in the concordance (3D) cosmology at $z = 0$ is only comparable to the 1D cosmology at $z = 1$ [1].

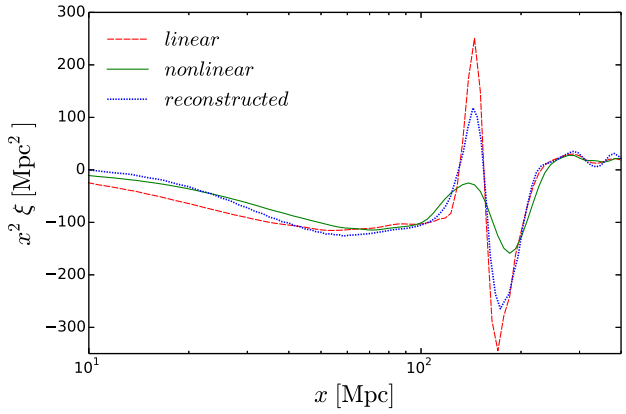

FIG. 1: The linear (dashed line), nonlinear (solid line), and reconstructed (dotted line) correlation functions. The distortion of the BAO peak is reduced by reconstruction.

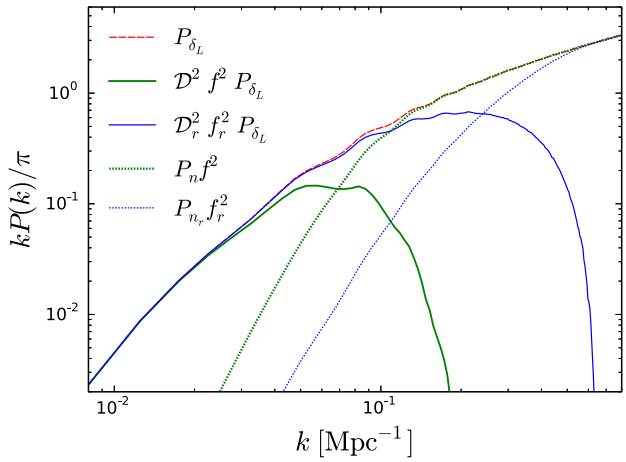

FIG. 2: The linear power spectrum (dashed line), the linear parts of the nonlinear (thick solid line) and reconstructed (thin solid line) power spectra, the noise parts of the nonlinear (thick dotted line) and reconstructed (thin dotted line) power spectra. For visual comparisions, we rescale both the linear and noise parts by $f^2 = P_{\delta_L}/P_\delta$ and $f_r^2 = P_{\delta_L}/P_{\delta_r}$ for the nonlinear and reconstructed fields, respectively. The noise terms dominate over the signals at $k \gtrsim 0.07$ Mpc^{-1} for the nonlinear field and $k_q \gtrsim 0.24$ Mpc^{-1} for the reconstructed field.

IV. RESULTS

Figure 1 shows the linear, nonlinear and reconstructed correlation functions. Since the BAO feature in 1D is sharper than that in 3D, the smearing of the BAO peak in 1D is more subtantial [1]. Nevertheless, the new reconstruction method sharpens the peak signigicantly. The nonlinear density field $\delta(x)$ is given on the Eulerian position x, while the reconstructed density field $\delta_r(q)$ is calculated on the Lagrangian position q.

To conveniently quantify the linear information δ_L in the nonlinear density field δ, we decompose the nonlinear

density field δ as

$$\delta(k) = b(k)\delta_L(k) + n(k). \quad (6)$$

Here, $b\delta_L$ is completely correlated with the linear density field δ_L. Correlating the nonlinear density field with the linear density field,

$$\langle\delta(k)\delta_L(k)\rangle = b(k)\langle\delta_L(k)\delta_L(k)\rangle, \quad (7)$$

we obtain

$$b(k) = \frac{P_{\delta\delta_L}(k)}{P_{\delta_L}(k)}. \quad (8)$$

Nonlinear evolution drives $b(k)$ to drop from unity, reducing the linear signal. Separating the part correlated with the linear density field, we have $n(k) = \delta(k) - b(k)\delta_L(k)$. $n(k)$ is generated in the nonlinear evolution and thus uncorrelated with the linear density field δ_L, further reducing $b\delta_L$ with respect to δ. This part induces noise in the measurement of BAO. Such decomposition helps to write the nonlinear power spectrum as

$$P_\delta(k) = \mathcal{D}(k)P_{\delta_L}(k) + P_n(k), \quad (9)$$

where $\mathcal{D}(k) = b^2(k)$ is the nonlinear damping factor. Here, $b(k)$ is often referred as the "propagator" and P_n is usually called the "mode-coupling" term [4–6]. For the reconstructed field $\delta_r(q)$, we also have

$$\delta_r(k_q) = b_r(k_q)\delta_L(k_q) + n_r(k_q), \quad (10)$$

where $b_r(k_q) = P_{\delta_r\delta_L}(k_q)/P_{\delta_L}(k_q)$. Similarly, the reconstructed power spectrum is given by

$$P_{\delta_r}(k) = \mathcal{D}_r(k)P_{\delta_L}(k) + P_{n_r}(k), \quad (11)$$

where $\mathcal{D}_r(k) = b_r^2(k)$. Here, the subscript "$q$" denotes that the reconstructed field is given on the Lagrangian coordinate. In Fig. 2, we plot the linear components and the noise terms of the nonlinear and reconstructed fields.

Figure 3 shows the damping factors for the nonlinear and reconstructed fields. The damping of the linear power spectrum is significantly reduced after reconstruction. We also overplot the best-fitting Gaussian BAO damping model,

$$\mathcal{D}(k) = \mathrm{e}^{-k^2\Sigma^2/2}, \quad (12)$$

with $\Sigma = 16.5$ Mpc and 4.9 Mpc for the nonlinear and reconstructed fields. The new BAO reconstruction algorithm reduces the nonlinear damping scale Σ by 70 percent. The damping factor for the reconstructed field is above 0.9 for $k \lesssim 0.1$ Mpc^{-1}. However, the 100 percent reconstruction, cancelling any nonlinear effects, is still unachievable, as some information has been irreversibly lost.

Reconstruction reduces the nonlinear damping $\mathcal{D}(k)$ as well as the noise term $P_n(k)$. To quantify the overall performance, we can use the cross-correlation coefficient

$$r(k) = \frac{P_{\delta\delta_L}(k)}{\sqrt{P_\delta(k)P_{\delta_L}(k)}} = \frac{1}{\sqrt{1+\eta(k)}}, \quad (13)$$

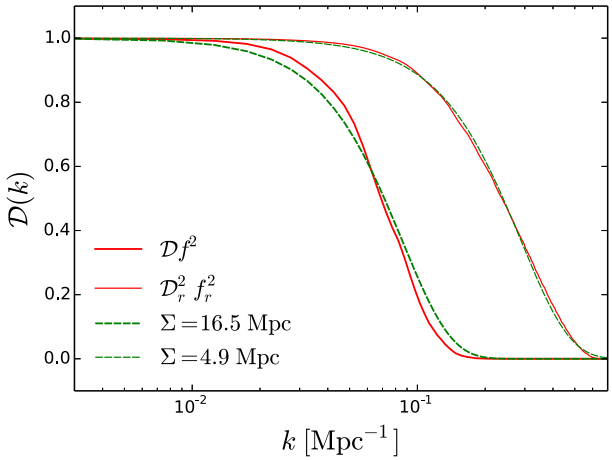

FIG. 3: The damping factors for the nonlinear (thick solid line) and reconstructed (thin solid line) fields. The Gaussian BAO damping models with $\Sigma = 16.5$ Mpc (thick dashed line) and $\Sigma = 4.9$ Mpc (thin dashed line).

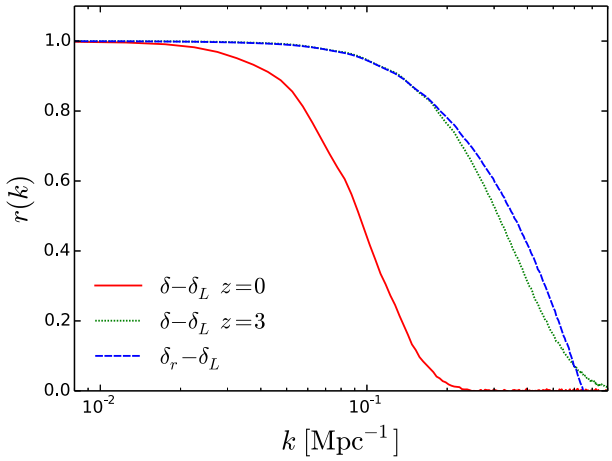

FIG. 4: The $\delta - \delta_L$ correlation coefficients at $z = 0$ (solid line) and $z = 3$ (dotted line), as well as the $\delta_r - \delta_L$ correlation coefficient (dashed line).

where $\eta = P_n/(b^2P_{\delta_L})$ quantifies the relative amplitude of n with respect to $b\delta_L$. We plot the cross-correlation coefficients in Fig. 4. The correlation of δ_r with δ_L is even better than that of δ at $z = 3$.

The raw reconstructed field δ_r is still noisy on small scales ($k_q \gtrsim 0.24$ Mpc^{-1}). To optimally filter out the noise from the raw reconstructed field, we use the Wiener filter

$$W_r(k_q) = \frac{P_{\delta_L}(k_q)}{P_{\delta_L}(k_q) + P_{n_r}(k_q)/b_r^2(k_q)}. \quad (14)$$

Deconvolving b_r and using the Wiener filter, we obtain the optimal reconstructed field,

$$\tilde{\delta}_r(k_q) = \frac{\delta_r(k_q)}{b_r(k_q)}W_r(k_q). \quad (15)$$

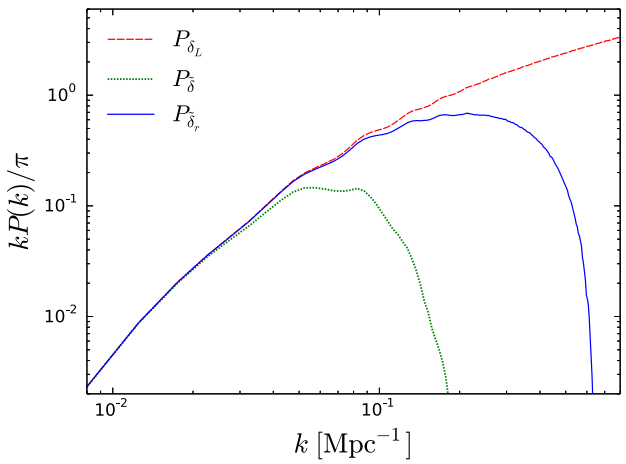

FIG. 5: The power spectra for the linear (dashed line), filtered nonlinear (dotted line) and filtered reconstructed (solid line) fields. The wiggles in the reconstructed power spectrum are much more apparent than the nonlinear power spectrum.

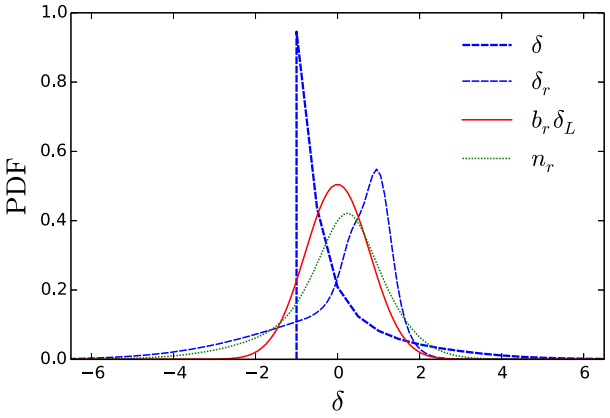

FIG. 6: The probability distribution functions of the nonlinear (thick dashed line) and reconstructed (thin dashed line) fields. We also show the PDFs of the linear component (solid line) and the noise part (dotted line). The PDFs are evaluated on $N_{\rm grid} = 6 \times 10^7$ grids, i.e., the grid scale is 5/3 Mpc.

The power spectrum of the optimal reconstructed field $\tilde{\delta}_r$ is given by

$$P_{\tilde{\delta}_r}(k_q) = W_r^2(k_q)P_{\delta_L}(k_q) + W_r^2(k_q)P_{n_r}(k_q)/b_r^2(k_q). \quad (16)$$

The raw nonlinear field δ is also filtered. In Fig. 5, we plot the power spectra of the optimal filtered reconstructed and nonlinear fields. The wiggles in the reconstructed power spectrum are much more apparent than the nonlinear power spectrum.

The density fluctuation probability distribution function (PDF) quantifies the Gaussianity of the density field. Figure 6 shows the PDFs of the nonlinear and reconstructed density fields. We also plot the PDFs of the linear component $b_r\delta_L$ and the noise part n_r of the reconstructed density field δ_r. Of course the linear component is Gaussian, while the noise part is nonGaussian. As a result, the reconstructed density field is also nonGaussian. The raw nonlinear density field is clearly nonGaussian.

V. DISCUSSIONS

The new reconstruction method successfully recovers the lost linear information on the mildly nonlinear scales (till $k \lesssim 0.24$ Mpc^{-1}). The result in 1D provides an intuitive view of the algorithm and motivates us to develop the reconstruction method in 3D. The nonlinear displacement beyond the Zel'dovich approximation in 3D can be solved using the multigrid iteration scheme [7]. The algorithm for solving the 3D nonlinear displacement is originally introduced for the adaptive particle-mesh N-body code [7] and the moving mesh hydrodynamic code [8]. The 3D case is also more complicated since the 3D displacement field involves a curl part (vorticity) which is generated after shell crossing, while this does not happen after particles cross over in 1D. This requires us to quantify the effect of vorticity, which can be accomplished using N-body simulations. By decomposing the simulated displacement field into a irrotational part and a curl part, we can study the statistical properties of different components [9, 10]. These will be presented in future.

The reconstructed nonlinear displacement field is also important for the current BAO reconstruction [2], where the linear continuity equation is adopted to solve the displacement under the Zel'dovich approximation. However, the nonlinear displacement retains much more information, describing the motion of dark matter fluid elements beyond the linear order. The reconstructed displacement field $s(q)$ is given on the Lagrangian coordinate instead of the final Eulerian coordinate. This helps to correct the effect due to the use of $s(x)$ instead of $s(q)$ in the BAO reconstruction [3, 11]. As more nonlinear effects will be removed using the nonlinear displacement, we expect the modeling of the reconstructed density field will be simplified.

The Wiener filter is optimal for the case both the signal and the noise are Gaussian random fields. In Fig. 6, the PDFs of the reconstructed density field and the noise are apparently nonGaussian. The reconstruction can be further improved using the nonlinear filter rather than the Wiener filter [12]. We plan to study this in future.

VI. ACKNOWLEDGEMENTS

We are very grateful to Matthew McQuinn for providing the 1D N-body simulations and helpful comments on the manuscript. We also thank Yu Yu, Tian-Xiang Mao and Wen-Xiao Xu for useful discussions. We acknowledge the support of the Chinese MoST 863 program under Grant No. 2012AA121701, the CAS Science Strategic Priority Research Program XDB09000000, the NSFC under Grant No. 11373030, IAS at Tsinghua University, and NSERC. The Dunlap Institute is funded through

an endowment established by the David Dunlap family and the University of Toronto. Research at the Perimeter Institute is supported by the Government of Canada through Industry Canada and by the Province of Ontario through the Ministry of Research & Innovation.

[1] M. McQuinn and M. White, J. Cosmology Astropart. Phys. **1**, 043 (2016), 1502.07389.
[2] D. J. Eisenstein, H.-J. Seo, E. Sirko, and D. N. Spergel, ApJ **664**, 675 (2007), astro-ph/0604362.
[3] M. Schmittfull, Y. Feng, F. Beutler, B. Sherwin, and M. Y. Chu, Phys. Rev. D **92**, 123522 (2015), 1508.06972.
[4] M. Crocce and R. Scoccimarro, Phys. Rev. D **73**, 063520 (2006), astro-ph/0509419.
[5] M. Crocce and R. Scoccimarro, Phys. Rev. D **77**, 023533 (2008), 0704.2783.
[6] T. Matsubara, Phys. Rev. D **77**, 063530 (2008), 0711.2521.
[7] U.-L. Pen, ApJS **100**, 269 (1995).
[8] U.-L. Pen, ApJS **115**, 19 (1998), astro-ph/9704258.
[9] P. Zhang, J. Pan, and Y. Zheng, Phys. Rev. D **87**, 063526 (2013), 1207.2722.
[10] Y. Zheng, P. Zhang, Y. Jing, W. Lin, and J. Pan, Phys. Rev. D **88**, 103510 (2013), 1308.0886.
[11] M. White, MNRAS **450**, 3822 (2015), 1504.03677.
[12] U.-L. Pen, Philosophical Transactions of the Royal Society of London Series A **357**, 2561 (1999), astro-ph/9904170.